УДК 621.7

Effect of excess Fe_2O_3 content on microstructure and tensile properties of 304 stainless steel with dual nanocrystalline and microcrystalline austenite prepared by aluminothermic reaction casting

Влияние избыточного содержания Fe_2O_3 на микроструктуру и свойства при растяжении нержавеющей стали 304 с двойным нанокристаллическим и микрокристаллическим аустенитом, полученным методом алюмотермического литья

Haibin Liu, Ying Wei, Peiqing La *, Yijun Han, Zhengning Li, Yu Shi

Х. Лю, И. Вэй, П. Ла *, И. Хан, Ч. Ли, Ю. Ши

State key Laboratory of Advance Processing and Recycling of Non-ferrous Metals, Lanzhou University of Technology, Lanzhou Gansu, 730050, China

* pqla@lut.cn

Государственная лаборатория инновационной обработки и переработки цветных металлов, Технологический университет Ланьчжоу, Китай, 730050, Ланьчжоу Ганьсу

* pqla@lut.cn

ABSTRACT

Microstructures of the 304 stainless steels, with nanocrystalline and microcrystalline austenite prepared by an aluminothermic reaction casting with different contents of Fe_2O_3 in reactants, have been investigated by XRD, SEM and EDS, and TEM. The results show that with the increase of the excessive content of Fe_2O_3 in the reactants, the content of Al remained in the steels decreased firstly and then increased, while the content of other alloying elements such as Cr, Ni decreased. When Fe_2O_3 was 5 wt.% in the reactants, the amount of Al and the ferrite content reached the minimum. The cast 304 austenitic stainless steel prepared with the excess Fe_2O_3 of 5wt% was mainly composed of microcrystalline, nanocrystalline austenite and a little microcrystalline ferrite. The volume fraction of the nanocrystalline austenite in the steel was about 67% when Fe_2O_3 was 5 wt.% in the reactants and the tensile strength of the cast steel was 674 MPa, the yield strength was 458 MPa, and the elongation rate was 10.4 %.

KEYWORDS

Aluminothermic reaction; 304 stainless steel; microstructure; tensile properties.

АННОТАЦИЯ

Микроструктуры нержавеющих сталей 304 с нанокристаллическим и микрокристаллическим аустенитом, полученным путем алюминотермического литья с различным содержанием Fe_2O_3 в реагентах, были исследованы методами рентгеноструктурного анализа, сканирующей электронной микроскопии, энергодисперсионной рентгеновской спектроскопии и просвечивающей электронной микроскопии. Результаты показывают, что с увеличением избыточного содержания Fe_2O_3 в реагентах содержание Al, оставшегося в сталях, сначала уменьшалось, а затем увеличивалось, тогда как содержание других легирующих элементов, таких как Cr, Ni, уменьшалось. Когда доля Fe_2O_3 в реагентах составляла 5 мас. %, количество Al и содержание феррита достигали минимума. Литая аустенитная нержавеющая сталь 304, приготовленная с избытком Fe_2O_3, состояла в основном из микрокристаллического, нанокристаллического аустенита и небольшого количества микрокристаллического феррита. Объемная доля нанокристаллического аустенита в стали составляла около 67 %, когда доля Fe_2O_3 составляла 5 мас. %. При этом предел прочности при растяжении отлитой стали составлял 674 МПа, предел текучести составлял 458 МПа, а степень удлинения составляла 10,4 %.

КЛЮЧЕВЫЕ СЛОВА

Алюминотермическая реакция; нержавеющая сталь 304; микроструктура; механические свойства.

Introduction

Due to the presence of fully austenite, austenitic stainless steels have good corrosion resistance, ductility, welding characteristics and non-magnetic properties [1–5]. Therefore, austenitic stainless steels have become one of the most attractive engineering alloys, widely used in chemical engineering, bioengineering, aerospace, nuclear energy and medical equipment and other fields [6]. The 304 austenitic stainless steel is one of the most common types of AISI 300 series, and its chemical

composition must meet the requirements of table 1. However, the low yield strength of the 304 stainless steel at room temperature limits its application in industry, which is still a major drawback of most austenitic stainless steel [7, 8]. In recent years, how to improve the strength of the 304 austenitic stainless steel has become an important issue/project for many researchers. Many studies have shown that there are different methods to heighten the strength of materials, such as solid solution strengthening, work hardening and grain refinement [9–12]. Among these methods, only grain refinement can effectively improve the material strength while improving the willfulness. The relationship between strength and grain size conforms to the Hall-Petch formula [13]. Other methods are aimed at sacrificing plasticity to enhance the strength.

Adding a certain amount of micro-crystals on the basis of maintaining nano-crystals, stainless steel with micro-nano structure can form micro-and nano-scale inhomogeneous structure, and it has excellent comprehensive mechanical properties. Hence, stainless steel with micro-nano structure has been broadly applied in some engineering fields [14, 15]. At present, the preparation methods of micro-and nano-structured metal materials mainly include severe plastic deformation [16], powder metallurgy (combustion synthesis) [17] and amorphous alloy crystallization method. In these different methods, researchers have successfully prepared carbon steels [18], pure copper [19, 20] and pure nickel with micro-nanostructures [21]. It has also been experimentally confirmed that the micro-nano structure with double-scale distribution can significantly increase the plasticity of nanocrystalline materials [22]. From the perspective of energy saving and industrial production amplification, combustion synthesis is one of the most promising methods for the preparation of these materials. The aluminothermic reaction used in this paper is a highly exothermic reaction, and the principle is the same as the self-propagating high-temperature synthesis method. Once the reaction begins, a large amount of heat released during the reaction will quickly drive the reaction zone to fully react, providing the necessary conditions for the formation of the entire sample [23]. The adiabatic temperature in the reaction system is much higher than the melting point of the product and the by-product alumina, and the high temperature makes the melt superheated and pure. The reacted melt is deposited directly on the copper substrate. The copper material has a large thermal conductivity, and the high cooling rate causes a large degree of subcooling, and thus stainless steel has a smaller critical nucleus size during solidification. The high nucleation rate and the low atomic diffusion rate ensure that the final solidified tissue has a smaller size.

Without using complicated process and expensive facilities, this study presents a novel and practical process for fabricating the 304 stainless steel using aluminothermic reactions of Fe_2O_3, Al, Cr, Mn, Si, C and Ni. Since Al is a stable ferrite phase element, the ferrite phase region can be expanded, which can lead to arise ferrite in austenitic stainless steel, and the 304 stainless steel is dominated by single phase austenite in industrial applications. Therefore, we hope that by increasing the amount of Fe_2O_3 in the reactant, Al powder in the aluminum thermal reaction can be fully reacted, so as to obtain the single-phase 304 austenite stainless steel.

1. Experimental techniques

1.1. Material preparation

The principle of the aluminothermic reaction is as follows:

$$Fe_2O_3 + 2Al = Al_2O_3 + 2Fe \qquad (1)$$

In this paper, Fe_2O_3, Al, Cr, Mn, Si, Ni, C powders were used as raw materials. The normal composition of each reactant was calculated in combination with the chemical composition of the 304 stainless steel in Table 1 and the equation (1) of the reaction. The content of Fe_2O_3 was overdosed by 2.5%, 5% and 7.5% (mass ratio) on the basis of the normal ratio to achieve the purpose of completely reacting Al powder. Table 2 shows the chemical composition of powders in different samples.

According to the requirements of table 2, mechanical milling of powder mixtures was performed by a QM-1SP4 planetary ball mill using some Al_2O_3 balls, with a ball to powder ratio of 1/2, a rotation speed of 180 RPM for 8h after weighing the raw materialsand mixing them evenly.

Table 1
Таблица 1

Chemical composition of 304 stainless steel
Химический состав нержавеющей стали марки 304

C(wt%)	Mn(wt%)	P(wt%)	S(wt%)	Si(wt%)	Cr(wt%)	Ni(wt%)	Fe(wt%)
≤0.08	≤2.00	≤0.045	≤0.030	≤1.00	18~20	8~10.5	Balance

Table 2
Таблица 2

Chemical composition of powders in the different series
Химический состав порошков различных серий

Sample name	Fe_2O_3(wt%)	Al (wt%)	Cr (wt%)	Mn (wt%)	Si (wt%)	Ni (wt%)	C (wt%)
A	61.05	20.6	11	1.2	0.6	5.5	0.05
B	62.576	20.6	11	1.2	0.6	5.5	0.05
C	64.103	20.6	11	1.2	0.6	5.5	0.05
D	65.629	20.6	11	1.2	0.6	5.5	0.05

Then, 300 g powder mixtures were weighed and placed in a self-made mold, which was a cylindrical block in a diameter of 85 mm, and pressed by a uniaxial press. The pressed block was put in a copper crucible, and a small ignition was set on the top of the reactants. After that, the crucible was placed and heated in an autoclave. After the synthesis process, a slag layer covered the main product of the synthesis. The connection between the slag layer and the product is weak and can be removed by hand tapping.

1.2. Characterization methods

By means of operating optical microscopy (OM, Mef3) and trans mission electron microscopy (TEM, JEM-2010) at 200 kV, microstructure characterization was performed. Also, X-ray diffraction (XRD, D/Max-2400) with Cu-Kα radiation was conducted to determine the phase composition of the samples. The scan angle was ranged from 20° to 130° with a speed of 10°/min. The tube voltage and the electrical current were 40 kV and 150 mA, respectively. The microstructures of the samples were analyzed by optical microscopy and scanning electron microscope (SEM, JSM-6700F) equipped with energy dispersive spectroscopy (EDS).

Cut from the main products, micro-tensile specimens fitted the required dimensions as illustrated in fig. 1. Uniaxial tensile testing was carried out on a WDW-100D electronic universal material testing machine. Also, by a HBRVU-187.5 optical hardness tester, the hardness of the samples was measured.

2. Results

2.1. Phase and microstructure analysis

The XRD patterns of the 304 stainless steel prepared by different amounts of Fe_2O_3 are depicted in fig. 2. Obviously, compared with the 304 stainless steel prepared by the normal ratio (sample A), it can be seen that when Fe_2O_3 is excessive (sample B, sample C and sample D), the diffraction peaks of ferrite are greatly weakened, and the main constituent phase is austenite. The excessive Fe_2O_3 eliminates the influence of Al element, and the amount of ferrite decreases significantly compared with the normal ratio. When Fe_2O_3 exceeds 5%, the ferrite content is the least, and the constituent phase is basically single-phase austenite. As the content of the excessive Fe_2O_3 reached 7.5%, the diffraction peaks of ferrite (211) increased slightly in the structure of the synthesized sample D.

Fig. 3 shows the optical micrographs of the 304 stainless steel prepared by different amounts of Fe_2O_3. It can be seen from the metallographic diagram that the microstructure is composed of two phases with different shades of color, and the light phase is the main one, which occupies more volume fraction, while the dark phase is mainly distributed at the interface of the light phase existing less content. The lighter white phase is the austenite phase of the matrix, while the ferrite phase is slightly darker and the proportion of the ferrite phase is small.

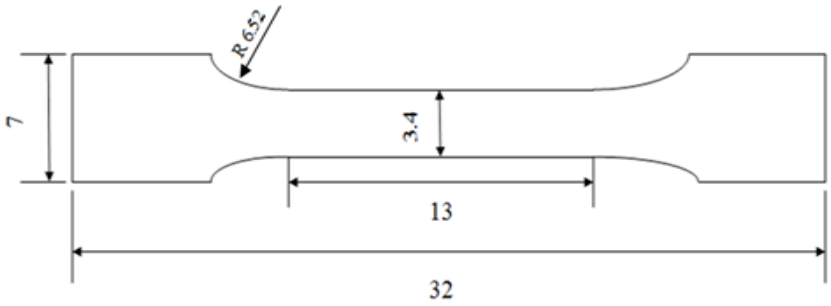

Fig. 1. The dimension of the tensile samples
Рис. 1. Измерение образцов на растяжение

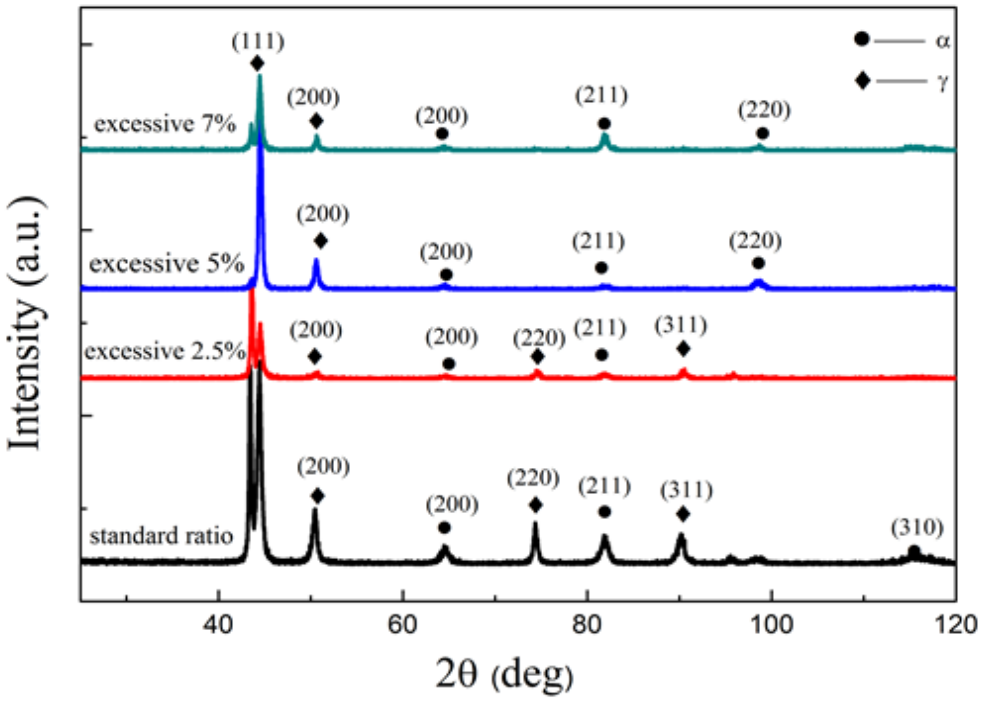

Fig. 2. The XRD patterns of the 304 stainless steel prepared by different amounts of Fe_2O_3

Рис. 2. Картины рентгенографии нержавеющей стали 304 с различным количеством Fe_2O_3

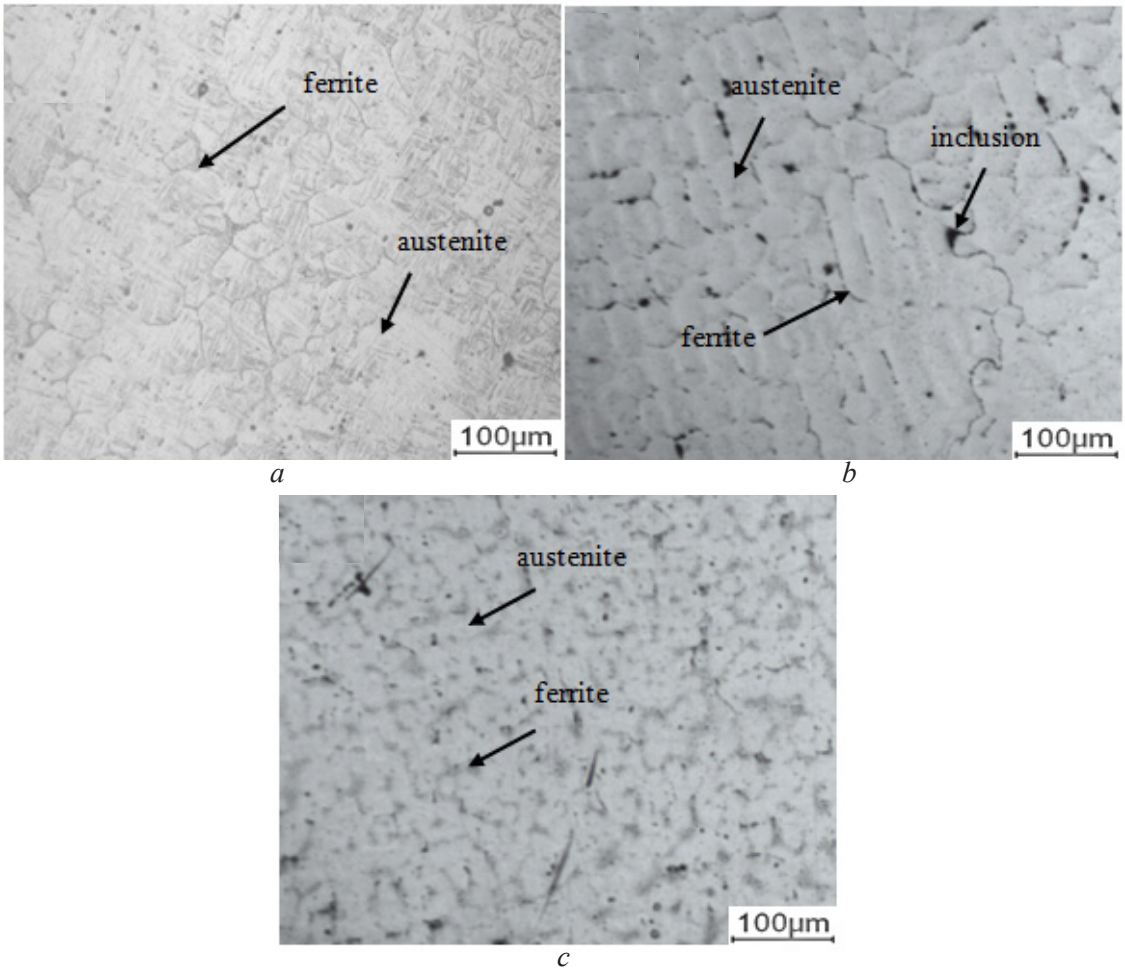

a *b*

c

Fig. 3. Metallographic structure of the 304 stainless steel prepared by different amounts of Fe_2O_3: *a* – 2.5%; *b* – 5%; *c* – 7.5%

Рис. 3. Металлографическая структура нержавеющей стали 304 с различным количеством Fe_2O_3: *a* – 2,5%; *b* – 5%; *c* – 7,5%

In the meantime, a small amount of inclusions can be seen from the metallographic phase. The XRD results show that the diffraction intensity of ferrite is weak, which indicates the content of ferrite is very small and the metallographic structure is consistent with the XRD results.

Fig. 4 shows the SEM images of the 304 stainless steel prepared by the excessive Fe_2O_3 differentiated between different content and EDS spectra of ferrite region. It is observed from the SEM structure that there is some ferrite distributed in the grain boundary matrix of matrix, and the matrix of the stainless steel is autensite. As the content of the excessive Fe_2O_3 reached 7.5%, there are some inclusions in the tissue of sample D. The results of the energy spectrum analysis shows the inclusions of MnS and Fe-Cr-S. According to the statistics, with the increase of the excess mass percentage of Fe_2O_3, the volume of ferrite decreases first and then increases. When the excess of Fe_2O_3 is 2.5%, 5% and 7.5%, the proportion of ferrite is 6%, 3% and 8% respectively. It can be seen that the amount of ferrite is very small. Although the addition of the excessive Fe_2O_3 can not completely remove ferrite, compared with the normal proportion of the 304 stainless steel, the reduction of the ferrite content is very remarkable.

The content of Al and Cr in the alloys, with different excess percentages of Fe_2O_3, is compared by EDS, as shown in fig. 5. It can be seen from the diagram that the content of Al goes up first and then goes down with the addition of Fe_2O_3, and the content of Al in the alloy decreases prominently compared with the normal ratio, indicating that the excess of Fe_2O_3 promotes more Al to participate in the reaction. When the excess of Fe_2O_3 is 2.5%, the content of Al reduces greatly in comparison with the normal proportioning. When the excess of Fe_2O_3 reaches 5%, the content of Al decreases, but the decreasing trend is relatively gentle. As the content of the excessive Fe_2O_3 reaches 7.5%, the content of Al rises again, and the content of Cr and Ni in steel begins to decline. During the experiment, we found that Fe_2O_3 was not the more the better. When the content of Fe_2O_3 is undue, the ferritic phase in tissue can be reduced, and the content of Al descends as well. However, when Fe_2O_3 is excessive to 7.5%, the content of Cr and Ni in steel decreases, and the reaction by-products contains a large number of unreacted Fe_2O_3, and the reaction becomes more difficult. EDS also shows that the content of Al is higher than that of Fe_2O_3 when Fe_2O_3 is excessive to 5%, which demonstrates the addition of more Fe_2O_3 not only does not promote more Al to participate in the reaction, but also increases the content of Al and that causes the waste.

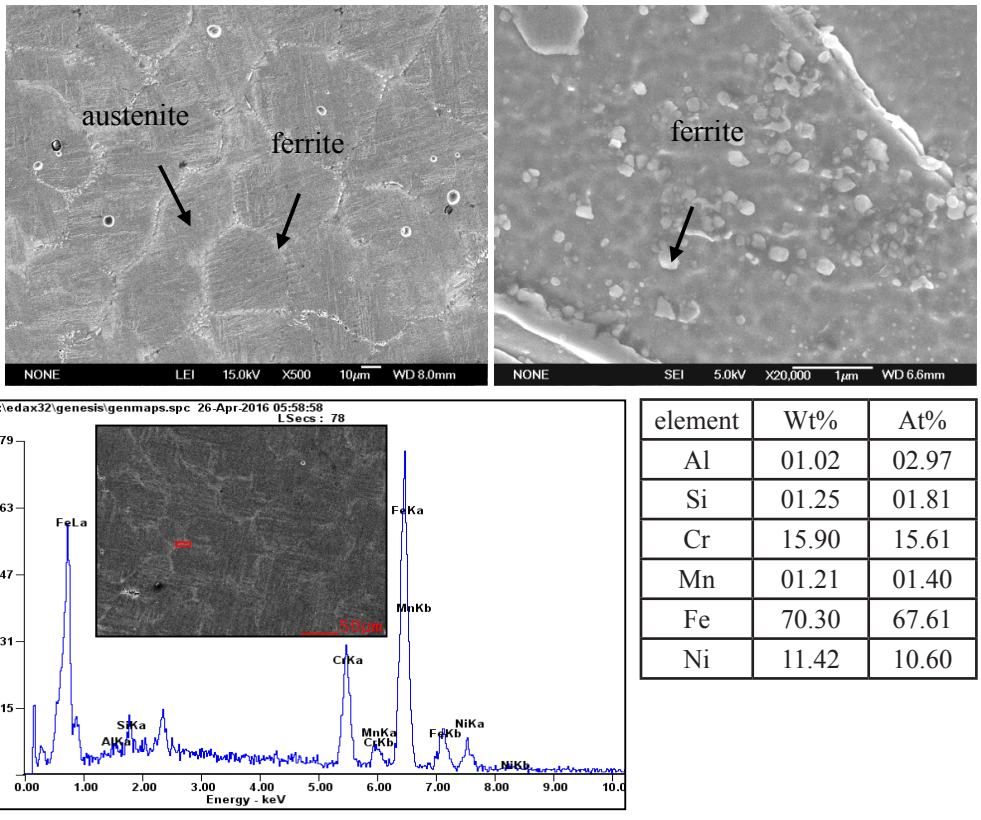

element	Wt%	At%
Al	01.02	02.97
Si	01.25	01.81
Cr	15.90	15.61
Mn	01.21	01.40
Fe	70.30	67.61
Ni	11.42	10.60

a

Fig. 4. SEM microstructure and EDS spectrums of the 304 stainless steel prepared by different amounts of Fe_2O_3: *a* – 2.5%

Рис. 4. Микроструктура (растровая микроскопия) и энергодисперсионные спектры нержавеющей стали 304 с различным количеством Fe_2O_3: *a* – 2,5%

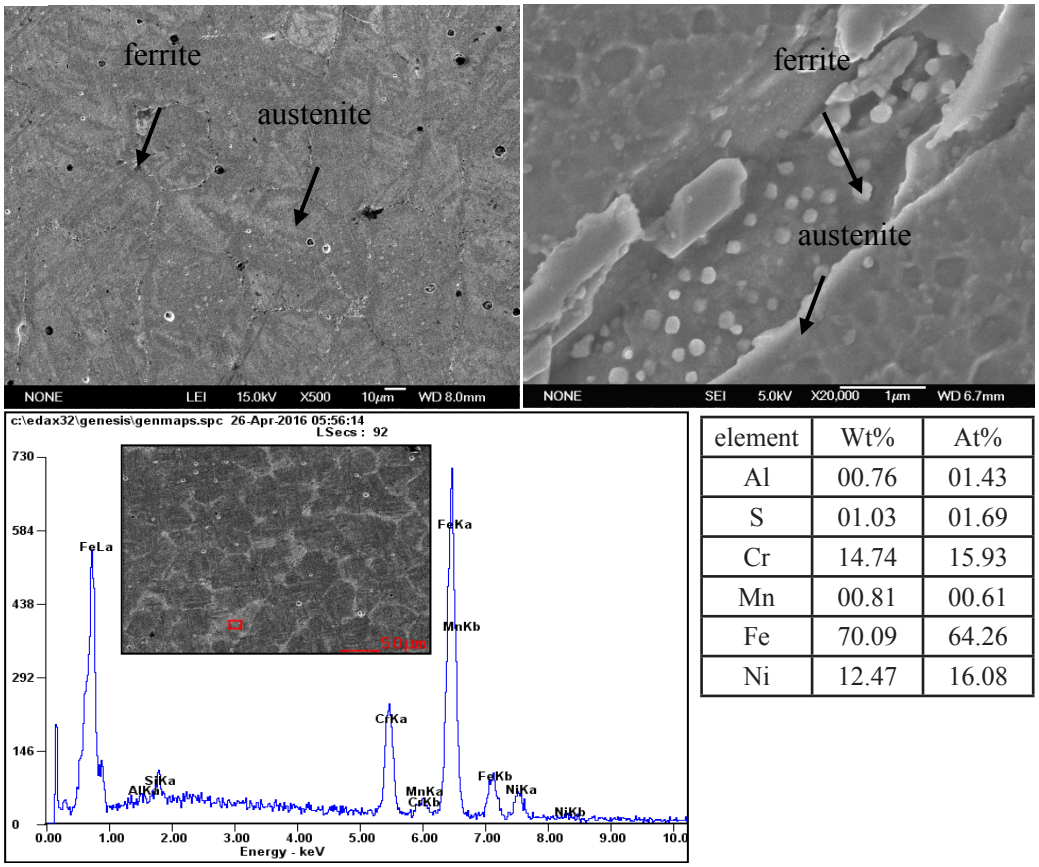

element	Wt%	At%
Al	00.76	01.43
S	01.03	01.69
Cr	14.74	15.93
Mn	00.81	00.61
Fe	70.09	64.26
Ni	12.47	16.08

b

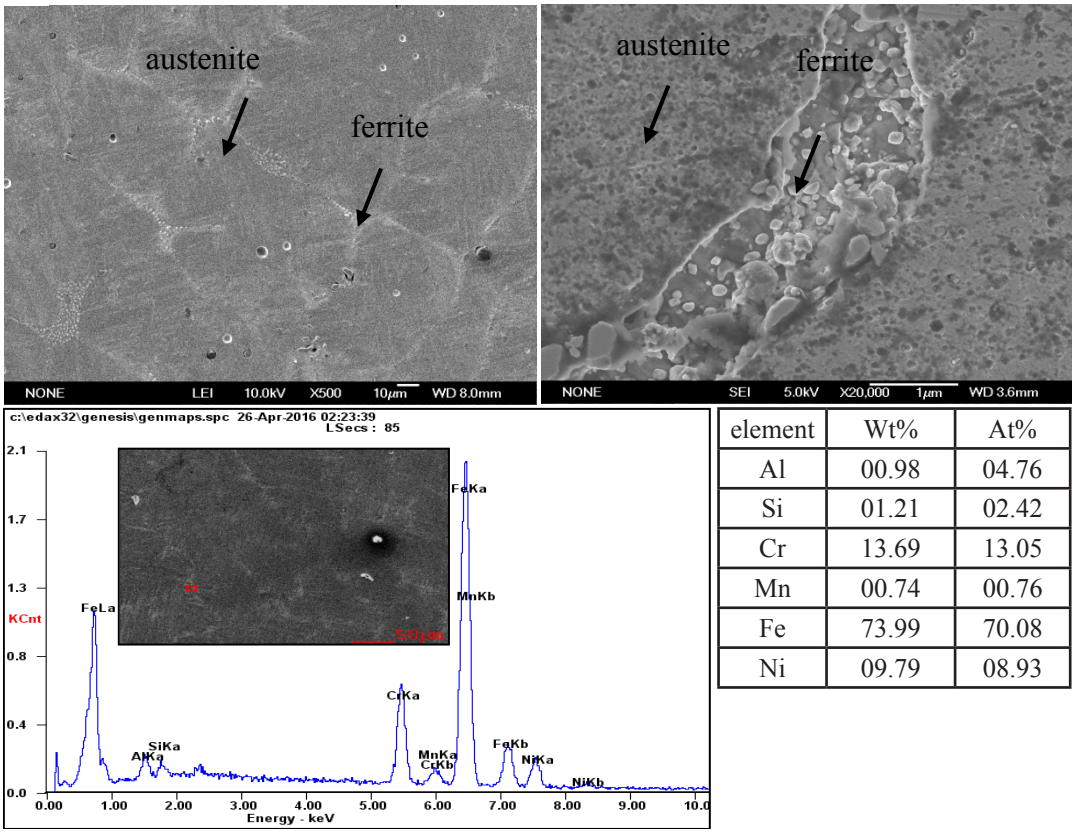

element	Wt%	At%
Al	00.98	04.76
Si	01.21	02.42
Cr	13.69	13.05
Mn	00.74	00.76
Fe	73.99	70.08
Ni	09.79	08.93

c

Fig. 4. SEM microstructure and EDS spectrums of the 304 stainless steel prepared by different amounts of Fe_2O_3: *b* – 5%; *c* – 7.5%

Рис. 4. Микроструктура (растровая микроскопия) и энергодисперсионные спектры нержавеющей стали 304 с различным количеством Fe_2O_3: *b* – 5%; *c* – 7,5%

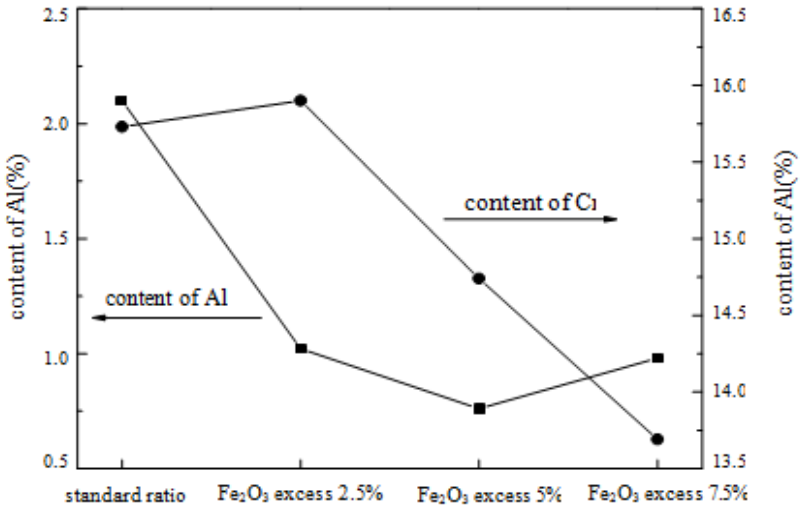

Fig. 5. The relationship curve of the content of Al and Cr in the alloys with different excess percentages of Fe_2O_3

Рис. 5. Кривая зависимости содержания Al и Cr в сплавах с различными избыточными долями Fe_2O_3

Fig. 6 shows bright field image, dark field image, selected area electron diffraction pattern of the 304 austenitic stainless steel prepared by a 5% excess of Fe_2O_3, and grain size statistical diagram of the nanocrystalline austenite. The bright areas in the bright field image of the transmission electron microscope do not diffract, and those black areas are diffracted correspond to the large-sized microcrystalline austenite; there are some light gray areas in the bright field image, corresponding to the white highlight areas in the dark field image. The selected area electron diffraction as a continuous ring indicates that there are many nanocrystals in the microstructure.

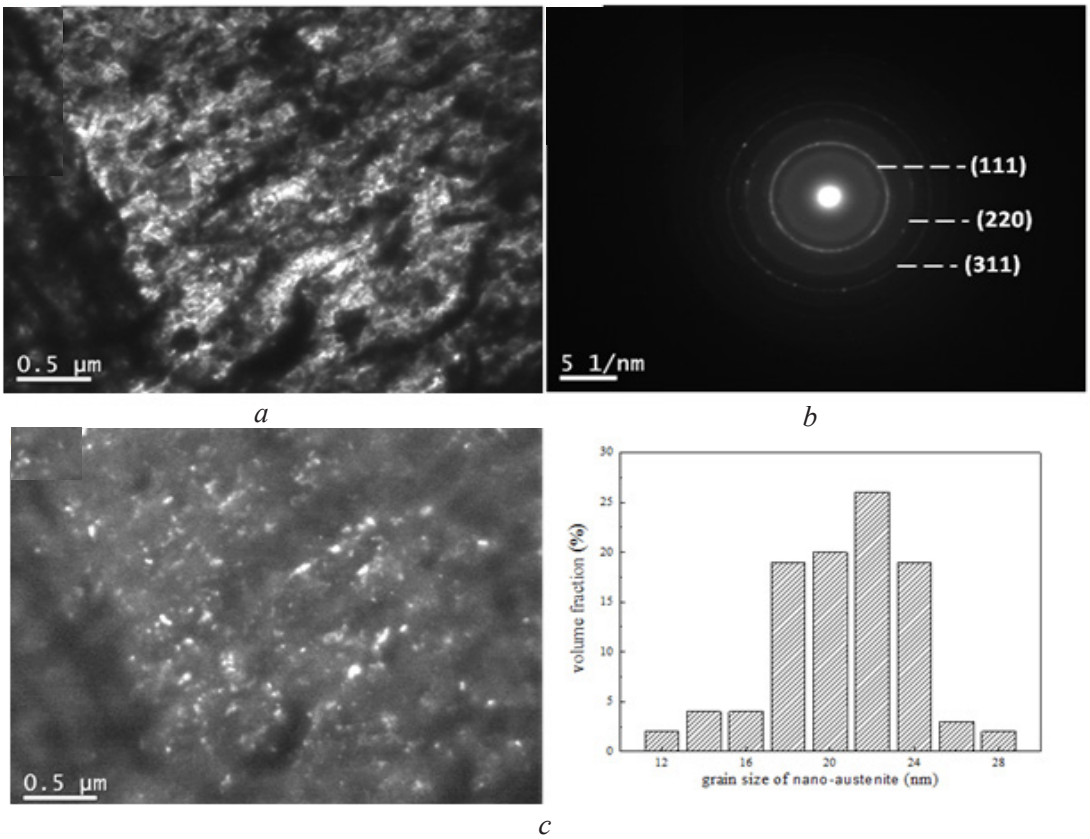

Fig. 6. TEM images of the 304 austenitic stainless steel prepared by a 5% excess of Fe_2O_3: *a* – bright field image; *b* – dark field image; *c* – selected area electron diffraction pattern; *d* – grain size statistical diagram of the nanocrystalline austenite

Рис. 6. Просвечивающая электронная микроскопия аустенитной нержавеющей стали 304, полученная с 5%-м избытком Fe_2O_3: *a* – светлопольное изображение; *b* – темнопольное изображение; *c* – выбранная область электронной дифракционной картины; *d* – размер зерна статистической диаграммы нанокристаллического аустенита

Because ferrite is not resistant to corrosion and can be corroded during the electrolysis process, it could not be observed in TEM. The Image Pro Plus software was used to calculate the amount of nanocrystalline austenite in the microstructure. The volume fraction of the nanocrystalline austenite was as high as 67% and the average grain size of the nanocrystalline austenite was about 21.9 nm.

Fig. 7 shows the tensile property curve and the hardness histogram of the 304 austenite stainless steel prepared with the normal proportion and over 5% of Fe_2O_3. It can be observed that the yield strength of the as-cast 304 stainless steel is lower, about 458 MPa, and the maximum tensile strength is 674 MPa, and the hardness value is 186HV when the excess of Fe_2O_3 is 5%. There is a plastic rheological zone before tensile fracture, but the elongation is still low, about 10.4%. The tensile properties and hardness are not distinctly different from those of the 304 stainless steel prepared at the earlier normal ratio.

3. Discussion

The alloy composition determines the solidification mode of the austenitic stainless steel. In order to investigate the solidification behavior of the austenitic stainless steel, some scholars simplified the complex alloy into Fe-Cr-Ni ternary alloy [24], and classified the solidification mode of the stainless steel according to the calculations of Cr and Ni equivalents:

(1) Model F: liquid phase L → liquid phase L and δ-ferrite → δ-ferrite → δ-ferrite and γ-austenite (Cr equivalent / Ni equivalent >1.95);

(3) Model FA: liquid phase L → liquid phase L and δ-ferrite → liquid phase L, γ-austenite and δ-ferrite → δ-ferrite and γ-austenite (1.48 < Cr equivalent / Ni equivalent <1.95);

(3) Model AF: liquid phase L → γ-austenite and liquid phase L → liquid phase L, γ-austenite and δ-ferrite → δ-ferrite and γ-austenite (1.25 < Cr equivalent / Ni equivalent <1.48);

(4) Model A: liquid phase L → γ-austenite and liquid phase L → γ-austenite (Cr equivalent / Ni equivalent <1.25).

In this paper, the calculations of Cr and Ni equivalent are as follows:

$Cr_{eq} = Cr + 1.5Si = 11.9$

$Ni_{eq} = Ni + 30C + 0.87Mn = 8.044$

The Cr equivalent / Ni equivalent = 1.478 < 1.48 belongs to model AF. That is to say, the primary phase precipitated in the liquid phase is austenite, and some ferrite forming elements is segregated at the austenite grain boundary when solidified like chromium or aluminum, which promotes the formation of ferrite at the grain boundary. Body, the nucleation of ferrite grows up surrounded by austenite. The second phase ferrite transforms to austenite during the late solid phase transformation, further reducing its number. Some studies have shown that the formation of cellular austenite in AF mode is associated with a high cooling rate [25]. Near equilibrium microstructure can be obtained at a low cooling rate, and full austenite or eutectic austenite can be acquired at a high cooling rate by inhibiting the precipitation of the second phase.

The Al element promotes the formation of the high-temperature delta ferrite, so that the solidified structure contains a certain amount of ferrite. The higher the content of Al, the more obvious this effect is.

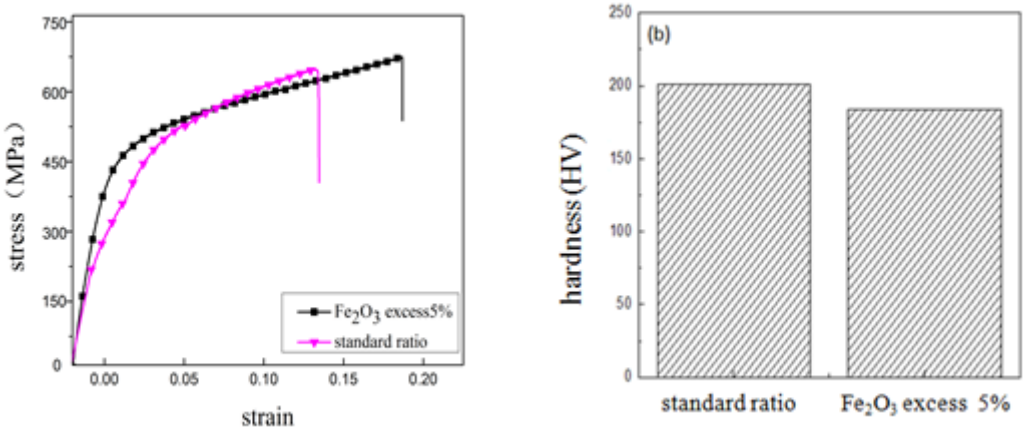

Fig. 7. The tensile property curve and the hardness histogram of the 304 austenite stainless steel prepared with the normal proportion and over 5% of Fe_2O_3

Рис. 7. Кривая растяжения и гистограмма твердости нержавеющей аустенитной стали 304, подготовленной с нормальной пропорцией и 5%-м переизбытком Fe_2O_3

However, the excessive Fe_2O_3 can make Al participate in the reaction as much as possible within a certain temperature range, reducing the precipitation of ferrite, which provides the possibility of obtaining single-phase austenite tissue. During the aluminum thermal reaction, the instantaneous release of high heat causes the whole system to react, and the reaction combustion wave spreads to the whole area from top to bottom, making the liquid melt get very good superheating purification. Therefore, during the late melt solidification process, the crystallization is carried out by homogeneous nucleation. At the beginning, the nucleation rate is low, and the content of alloy elements such as Cr, N, and Ni in the melt is very high, which provides energy fluctuation and composition fluctuation for the formation and growth of some nucleus. This part of the nucleus are preferentially grown into micron crystals after solidification. As the temperature decreases, when the degree of subcooling reaches a certain value, the nucleation rate rises rapidly, so much the critical nucleus radius reaches the minimum value, and the melt viscosity rises at a high cooling rate, which results in atomic diffusion hindered and would be limited. With the growth rate of the nucleus, after the solidification, this part of the nucleus forms a nanocrystal. The liquid oxide and the alloy are incompatible with each other and the density is much different, so the alumina and Fe_2O_3 which are not involved in the reaction are separated around the main product.

Aluminothermal reaction is a reaction that gives off a great deal of heat instantaneously. The reaction is characterized by high temperature and high speed. Therefore, this process can be regarded as an equilibrium process. As the amount of Fe_2O_3 increases, the content of Al gradually decreases, resulting in the reduction of heat release in the aluminum thermal system and the decrease of adiabatic temperature of the system. A large number of ferric oxide remains in the by-products. The microstructure observation and composition analysis shows that through ferric oxide excessively increasing, inclusions appears in the structure, and the inclusions are mainly manganese sulfide and Fe-Cr-S compounds. EDS analysis also reveals that with the increase of Fe_2O_3 content, the content of alloy elements is on the low side. By 7.5% ferric oxide excess, the content of Cr in ferrite phase of the alloy could be reduced to 13.69%. It is observed that the diffusion rate of elements reduces with the decrease of system temperature, and some alloy elements could not be completely melted into the matrix, which affects the microstructure, stability and uniformity. With the increasing of Fe_2O_3 content, the content of Al does not show a monotonous downward trend, which is related to the decline of the whole system temperature but not the completeness of the reaction. The as-cast 304 stainless steel prepared by the aluminothermic reaction method is a multi-dimensional composite structure composed of nanocrystalline austenite, microcrystalline ferrite and austenite, but the distribution of the micro-nano composite structure is not very uniform and continuous. Among them, the nanocrystalline austenite accounts for a large volume fraction, but the nanocrystals exhibits a cluster-like distribution on the microcrystalline matrix. Thus, the micro-nano composite structural material has a certain strength, but the dislocation storage capacity in the nanocrystal is limited. The work hardening ability is very weak. It cannot be well regulated among the ratio, grain size and distribution of nanocrystalline austenite and microcrystalline austenite in the as-cast micro-nanostructure 304 stainless steel. Therefore, the obtained as-cast micro-nano-structured stainless steel has low strength, low plasticity, and comprehensive mechanical properties deviation, and further comprehensive mechanical properties need to be gained by adjusting the ratio of microcrystalline and nanocrystalline, grain size and distribution state.

Conclusion

In this study, the 304 austenite stainless steel with micro-nano structure was prepared by adding different amounts of Fe_2O_3, and its tissue-related mechanical properties were characterized. The following conclusions were obtained:

1. The 304 stainless steel is mainly austenite when the excess of Fe_2O_3 is 2.5; 5 and 7.5%, which contains a small amount of ferrite, and the ferrite content reaches the minimum when the excess of Fe_2O_3 is 5%.

2. With the increase of the excess ratio of Fe_2O_3, the content of Al in the alloy decreases first and then rises, and the content of other alloying elements such as Cr and Ni reduces.

3. The as-cast 304 austenitic stainless steel prepared by over 5% Fe_2O_3 is mainly composed of micron crystalline ferrite, austenite and nanocrystalline austenite, of which the volume fraction of nanocrystalline austenite is up to 67%.

4. The as-cast 304 austenitic stainless steel prepared with excessive 5% Fe_2O_3 has low mechanical properties, with its maximum tensile strength of 674 MPa, yield strength of 458 MPa and elongation rate of about 10.4%.

References

1. Erosion–corrosion behaviour and corrosion resistance of AISI 316 stainless steel in flow jet impingement / Y. Zhao et. al. // Wear. 2015. V. 328–329. P. 464–474. DOI: 10.1016/j.wear.2015.03.017.

2. Washko S. D., Aggen G. ASM Handbook Vol 1: Properties and Selection, 3rd ed. ASM International, New York. 2005. P. 1303.

3. Multi-objective optimization of machining parameters during dry turning of AISI 304 austenitic stainless steel using grey relational analysis / S. K. Nayak et. al. // Procedia Mater. Sci. 2014. V. 6. P. 701–708.

4. Phase stability of AISI 304 stainless steel during sliding wear at extremely low temperatures / W. Hübner et. al. // Wear. 2003. V. 255, No. 1–6. P. 476–480.

5. Mechanical properties of austenitic stainless steel 304L and 316L at elevated temperatures / R. K. Desu et. al. // J. Mater. Res. Technol. 2015. V. 5, No. 1. P. 13–20. DOI: 10.1016/j.jmrt.2015.04.001.

6. Lo K. H., Shek C. H., Lai J. K. L. Recent developments in stainless steels // Mater. Sci. Eng. R. 2009. V. 65, No. 4–6. P. 39–104.

7. Some strengthening methods for austenitic stainless steels / L. P. Karjalainen et. al. // Steel Res. Int. 2008. V. 79, No. 6. P. 404–412.

8. Effect of large strain cold rolling and subsequent annealing on microstructure and mechanical properties of an austenitic stainless steel / I. Shakhova et. al. // Mater. Sci. Eng.: A. 2012. V. 545. P. 176–186.

9. Revealing extraordinary intrinsic tensile plasticity in gradient nano-grained copper / T. Fang et. al. // Scinece. 2011. V. 311, No. 6024. P. 1587−1590.

10. Kou H., Lu J., Li V. High-Strength and High-Ductility Nanostructured and Amorphous Metallic Materials // Advanced Materials. 2014. V. 26, No. 31. P. 5518−5524.

11. Lu K. The future of metals // Science. 2010. V. 328, No. 5976. P. 319−320.

12. Lu K., Lu L., Suresh S. Strengthening materials by engineering coherent internal boundaries at the nanoscale // Science. 2009. V. 324, No. 5925. P. 349−352.

13. On the validity of the Hall-Petch relationship in nanocrystalline materials [J] / A. H. Chokshi et. al. // Scripta Metallurgica. 1989. V. 23, No. 10. P. 1679−1683.

14. Paradox of strength and ductility in metals processed by severe plastic deformation / N. Tsuji et. al. // J. Materials Transaction. 2004. V. 45, No. 7. P. 2272−2281.

15. High tensile ductility in a nanostructured metal / Y. Wang et. al. // J. Nature. 2002. V. 419, No. 6910. P. 912−915.

16. Valiev R. Nanostructuring of metals by severe plastic deformation for advanced properties // J. Nature Materials. 2004. V. 3, No. 8. P. 511–516.

17. Fabrication of in situ Al2O3 reinforced nanostructure 304 stainless steel matrix composite by self-propagating high temperature synthesis process / J. Feizabadi et. al. // J. Materials & Design. 2015. V. 84. P. 325−330.

18. Hosseini S. M., Najafizadeh A., Kermanpur A. Producing the nano/ultrafine grained low carbon steel by martensite process using plane strain compression // Journal of Materials Processing Technology. 2011. V. 211, No. 2. P. 230−236.

19. Ramtani S., Dirras G., Bui H. Q. A bimodal bulk ultra-fine-grained nickel: Experimental and micromechanical investigations // J. Mechanics of Materials. 2010. V. 42, No. 5. P. 522−536.

20. High tensile ductility and strength in bulk nanostructured nickel / Y. Zhao et. al. // J. Advanced Materials. 2008. V. 20, No. 16. P. 3028−3033.

21. Revealing extraordinary intrinsic tensile plasticity in gradient nano-grained copper / T. H. Fang et. al. // J. Science. 2011. V. 331, No. 6024. P. 1587−1590.

22. Valiev R. Z., Islamgaliev R. K., Alexandrov I. V. Bulk nanostructured materials from severe plastic deformation // J. Progress in Materials Science. 2000. V. 45, No. 2. P. 103−189.

23. Sharifitabar M., Vahdati Khaki J., Haddad Sabzevar M. Effects of Fe additions on self ropagating high temperature synthesis characteristics of TiO2-Al-C-Fe system // Int. J. Self-Propag. High-Temp. Synth. 2014. V. 47. P. 93–101.

24. Schino D. Solidification mode and residual ferrite in low-Ni austenitic stainless steels // J. Journal of Materials Science. 2000. V. 35, No. 2. P. 375−380.

25. Alexandrov B. T. Single Sensor Differential Thermal Analysis of Phase Transformations and Structural Changes During Welding and Postweld Heat Treatment // J. Welding in the World. 2013. V. 51, No. 11. P. 48−59.